An improved finite element model of incremental forming using conic programming

Ankor Raithatha and Stephen Duncan

Abstract— **Incremental Sheet Forming (ISF) is a flexible method for forming sheet metal that can be considered as an incremental deformation process. A fast method for modeling deformation in ISF is required that can form the basis of a path optimisation and feedback control algorithm for the process. This paper improves upon previous formulations for approximately modeling ISF by incorporating bending work and using finite element discretisation. The model is solved by manipulating the problem into the form of a second-order cone program (SOCP) and significant improvements are observed in terms of numerical stability of the model allowing a full product to be simulated. For validation purposes, a comparison is provided between the new model and measured data.**

I. INTRODUCTION

Incremental deformation is a process that applies a series of small deflections to a material that accumulate to produce a large final deformation. Interest in the modelling of incremental deformation has increased over the past decade with the advent of a range of novel manufacturing techniques that automate the incremental deformation process, allowing shaped parts to be produced without the need for stamping. These processes, which are collectively referred to as Incremental Sheet Forming (ISF) [1], require no specialised tooling making them highly attractive for low volume manufacturing and rapid prototyping, both economically and in terms of flexibility [2]. The most general ISF process uses one small indenter that is pushed into the metal by 0.2-2 mm, causing plastic deformation. The indenter, which is 5-20 mm in diameter at the tip, is dragged over the sheet at this depth using a CNC sequence to create a small track. This is the first contour of the desired product. The tool then indents further and is tracked around to form the next contour of the part, and so on until the desired shape is built up.

Although ISF offers more flexibility compared to stamping processes, currently ISF does not produce components with sufficient accuracy. ISF processes are subject to several non-linear disturbances, such as elastic spring-back, metal work-hardening and stretching of the ISF machinery, all of which must be accounted for in order to ensure that the formed sheets agree well geometrically with the desired product. This is particularly of importance in manufacturing and medical applications. The aim of this work is to facilitate the development of a feedback control system that regulates the geometric accuracy of deformation over the plane of the sheet. To design such a system, a computationally efficient process model is required and is currently under development. Earlier progress on the work is described in [3] and [4], where the authors formulated a model for incremental forming using second-order cone programming (SOCP) under the assumption of rigid perfectly plastic material behaviour. The model used finite differencing for spatial discretisation and only the stretching component of work within the sheet was modeled. In [4], some preliminary results in modeling a CNC ISF process were presented. However, when modeling a full incrementally formed product, the proposed model was found to be numerically unstable except for very small time increments. Motivated by the successful application of the assumption of rigid plastic material behaviour in producing efficient models for other metal forming processes [5], the new model continues to use the assumption, but it is otherwise completely reformulated. The new model displays much better stability and is used to produce a full scale model of a part, which is then validated against measurements from a real product formed by ISF. The model also continues to use SOCP as the solution method, which is solved efficiently using state-of-the-art SOCP software. Furthermore, by the application of Ilyushin theory, the model now accounts for both membrane and bending effects within the sheet.

II. THE MODEL

The rigid perfectly plastic deformation assumption is still commonly used in the field of limit analysis in civil engineering, and it is there that it has seen the most recent development [6]. The model presented here therefore borrows some methods from limit analysis theory. Limit analysis is a basis for computing an estimate of the value of a multiplier that must be applied to a load distribution over a solid, under the assumption of rigid plastic deformation, in order to cause collapse [7]. Since the exact value of this multiplier is difficult to compute, the upper and lower bound methods are often used to provide the range of values it may take. The upper bound approach is applied here since for incremental deformation the material must undergo collapse in order to achieve the required deformation. It is therefore more appropriate to overestimate the multiplier and guarantee collapse, rather than to use the lower bound method and underestimate the limit load. It is noted that unlike in limit analysis, the deformation field of the material is of a greater interest here than the accurate computation of the value of the load multiplier.

A. Raithatha is with the Department of Engineering Science, University of Oxford, UK `ankor.raithatha@eng.ox.ac.uk`

S. Duncan is with the Department of Engineering Science, University of Oxford, UK `stephen.duncan@eng.ox.ac.uk`

A. Plate problem

The membrane and bending effects of the sheet are treated separately and superimposed. The latter, known as the plate formulation, will be provided first. Two important assumptions will be made: firstly, stresses normal to the surface of the sheet are considered to be negligible; secondly, under Kirchoff assumptions, only the deflections normal to the surface of the sheet are considered to be significant. Using stress resultant notation, the energy dissipation within the material due to bending moments is given as an integration over the surface of the sheet

$$D_e = \int_A M_x \dot{\kappa}_x + M_x \dot{\kappa}_y + M_{xy} \dot{\kappa}_{xy} \ \mathrm{d}A, \qquad (1)$$

where M_i are the bending moments defined as the through thickness integration of the product the stresses, σ_i, and the distance perpendicular to the plane of the sheet z,

$$M_i = -\int_z z \sigma_i \mathrm{d}z, \quad i = x, y, xy. \qquad (2)$$

The curvature rates $\dot{\kappa}_i$ are work conjugate to the bending moments,

$$\dot{\kappa}_x = \frac{\partial^2 w}{\partial x^2}, \quad \dot{\kappa}_y = \frac{\partial^2 w}{\partial y^2}, \quad \dot{\kappa}_{xy} = 2\frac{\partial^2 w}{\partial x \partial y}, \qquad (3)$$

where w is the transverse rate of deformation, or velocity, of the sheet.

If rigid plastic material behaviour without work-hardening is assumed, the stress distributions are rectangular during yield and the stress resultants are given by

$$M_i = \sigma_i \frac{h^2}{4}, \quad i = x, y, xy, o, \qquad (4)$$

where σ is the material yield stress and h is the sheet thickness. It is assumed that the non-linearity in material behaviour can be described using J_2 plasticity, so that the stresses are bound by the von Mises yield surface,

$$f(M_x, M_y, M_{xy}) = M_x^2 - M_x M_y + M_y^2 + 3M_{xy}^2 - M_o^2, \quad (5)$$

where $f(M_x, M_y, M_{xy}) = 0$ at yield, or by normalising the stress resultants by M_0 so that $m_x = \frac{M_x}{M_0}$, etc,

$$f(m_x, m_y, m_{xy}) = m_x^2 - m_x m_y + m_y^2 + 3m_{xy}^2 - 1$$
$$= \mathbf{m}^T \mathbf{H} \mathbf{m} - 1, \qquad (6)$$

where $\mathbf{m} = [m_x \ m_y \ m_{xy}]^T$ and $\mathbf{H}$ is symmetric positive definite. Defining the factorisation, $\mathbf{H} = \mathbf{C}^{-1}\mathbf{C}^{-T}$, and $\boldsymbol{\kappa} = [\dot{\kappa}_x \ \dot{\kappa}_y \ \dot{\kappa}_{xy}]^T$, the internal dissipation, D_e, under von Mises plasticity can be written as the integration over area of a norm of a linear function with respect to curvature,

$$D_I = M_0 \int_A ||\mathbf{C}\boldsymbol{\kappa}|| \mathrm{d}A, \qquad (7)$$

where the subscript I is used instead of e to emphasise that the allowable stress state is bound by the yield criterion. This

can be derived from the principle of maximum plastic work, from which the integrand of D_I in (7) is defined as

$$d_I = \max_{\mathbf{m}^T \mathbf{H} \mathbf{m} \leq 1} \mathbf{m}^T \boldsymbol{\kappa},$$
$$= \max_{||\mathbf{C}^{-T}\mathbf{m}|| \leq 1} \mathbf{m}^T \boldsymbol{\kappa}, \qquad (8)$$

the dual of which, in terms of dual variables λ, is

$$d_I = \min_{\lambda \geq 0} \quad \frac{1}{4\lambda} \boldsymbol{\kappa}^T \mathbf{H}^{-T} \boldsymbol{\kappa} + \lambda. \qquad (9)$$

The minimisation is performed by setting the derivative with respect to λ of the above to zero,

$$\lambda = \frac{1}{2} (\boldsymbol{\kappa}^T \mathbf{H}^{-T} \boldsymbol{\kappa})^{\frac{1}{2}} = \frac{1}{2} ||\mathbf{C}\boldsymbol{\kappa}||, \qquad (10)$$

where $\mathbf{H}^{-1} = \mathbf{H}^{-T} = \mathbf{C}^T \mathbf{C}$. The final result is obtained by back substituting (10) into (9),

$$d_I = \frac{2}{4} \frac{\boldsymbol{\kappa}^T \mathbf{H}^{-T} \boldsymbol{\kappa}}{||\mathbf{C}\boldsymbol{\kappa}||} + \frac{1}{2} ||\mathbf{C}\boldsymbol{\kappa}||,$$
$$= ||\mathbf{C}\boldsymbol{\kappa}||. \qquad (11)$$

1) Discretisation: The transverse velocity $w(x, y)$ is discretised by a cubic field in the form of the 9 degrees of freedom triangular BCIZ element, which is described in detail in [8]. There are several other choices of elements that present the required characteristics for discretising the model, but it is not the purpose of this paper to compare these. The element has nodes only at the vertices and three variables, w_i, $\frac{\partial w_i}{\partial y}$ and $-\frac{\partial w_i}{\partial x}$, are stored at each node, where i refers to the node number, 1, 2, or 3. Hermitian interpolation is used to approximate the value of $w(x, y)$ at any point within the element. The interpolation field is cubic with additional bubble functions and is given by the shape functions provided in [9]. Through differentiation of the appropriate shape functions, a relationship between the curvature and the nodal variables $\mathbf{w}$ is produced in the form of a linear matrix relationship. For a particular node i within an element, the curvature is given by

$$\boldsymbol{\kappa}_i^{(e)} = \mathbf{B}_{\mathrm{P},i}^{(e)} \mathbf{w}, \qquad (12)$$

where $\mathbf{B}_{\mathrm{P},i} \in \mathbb{R}^{3 \times NV}$ contains the coefficients of the relationship, NV is the number of variables and $\mathbf{w} \in \mathbb{R}^{NV}$ contains all the degrees of freedom over the sheet. The subscript P is used to emphasise that $\mathbf{B}$ is derived from plate theory, and superscripts, (e), refer to element number. The expression for curvature in equation (12) can be used to calculate the integrand in equation (7) at the nodes, since $||\mathbf{C}\boldsymbol{\kappa}_i|| = ||\mathbf{C}\mathbf{B}_{\mathrm{P},i}\mathbf{w}||$. An exact integration of $||\mathbf{C}\boldsymbol{\kappa}||$ over the area of the element would be costly in terms of numerical efficiency. An approximate integral is calculated instead by using the values of the integrand, $||\mathbf{C}\boldsymbol{\kappa}||$, at the nodes and restricting it to vary linearly over the element,

$$||\mathbf{C}\boldsymbol{\kappa}|| \approx L_1 ||\mathbf{C}\boldsymbol{\kappa}_1|| + L_2 ||\mathbf{C}\boldsymbol{\kappa}_2|| + L_3 ||\mathbf{C}\boldsymbol{\kappa}_3||, \qquad (13)$$

so that the integration of equation (13) over the element becomes

$$\int_A ||\mathbf{C}\boldsymbol{\kappa}|| \mathrm{d}A \approx \frac{\Delta}{3} (||\mathbf{C}\boldsymbol{\kappa}_1|| + ||\mathbf{C}\boldsymbol{\kappa}_2|| + ||\mathbf{C}\boldsymbol{\kappa}_3||), \qquad (14)$$

where Δ is the triangle area. This approximation always results in a value greater than or equal to the true value of the integration ensuring an upper bound solution. The discretised expression for internal dissipation over the sheet is a sum of norms,

$$D_I = \frac{M_0}{3} \sum_{e}^{NE} \sum_{i=1}^{3} \Delta \|\mathbf{CB}_{\mathrm{P},i}\mathbf{w}\|, \tag{15}$$

where NE is the total number of elements in the finite element mesh. It is convenient to stack the matrices $\mathbf{B}_{\mathrm{P},i}$ into a single sparse matrix $\mathbf{B}_{\mathrm{P}} \in \mathbb{R}^{9NE \times NV}$. By the principle of virtual work, the velocity field that minimises the internal dissipation provides the dynamical path of the system. For the first step of an incremental sheet forming process, the sheet metal is clamped at the edges and a tool of spherical surface indents the sheet at a single point, which leads to

$$\min_{\mathbf{w}} \; D_I,$$
$$\text{s.t. } \mathbf{w}_{tool} \geq \text{Tool surface function,}$$
$$\mathbf{w}_{boundary} = 0. \tag{16}$$

$\mathbf{w}_{boundary} \subset \mathbf{w}$ are the set of variables that are constrained at the boundaries. These can be implemented implicitly by removing the corresponding variables from the optimisation. The tool surface function describes the tool height at any position (x,y). The function produces a vector $\mathbf{t} \in \mathbb{R}^{NT}$ of the tool height at positions over the tool surface that coincide with nodes of the finite element mesh. The deformation variables $\mathbf{w}_{tool} \subset \mathbf{w}$ also correspond to these nodes. The above sum of norms problem can be rearranged into an optimisation problem with a linear objective function and quadratic conic constraints. Hence, the SOCP form of the above optimisation problem is obtained, with the introduction of two vectors of slack variables, $\boldsymbol{\eta} \in \mathbb{R}^{9NE}$ and $\mathbf{z} \in \mathbb{R}^{3NE}$, as

$$\min \; \mathbf{f}^T \mathbf{z}$$
$$\text{s.t. } \mathbf{Ew} \geq \mathbf{t}$$
$$\mathbf{CB}_{\mathrm{P}}\mathbf{w} = \boldsymbol{\eta}$$
$$\|\boldsymbol{\eta}_i\| \leq z_i \qquad i = 1,..,3NE, \tag{17}$$

where the clamping constraints are implicit, the vector $\boldsymbol{\eta}_i = [\eta_{1+3(i-1)}, \dots, \eta_{3i}]$, η_i and z_i are individual elements of their corresponding vectors and $\mathbf{Ew} = \mathbf{w}_{tool}$. From (15), the vector $\mathbf{f}$ contains elements that all have a value of $\frac{M_0}{3}$. Note that Δ in equation (15) has been incorporated into $\mathbf{B}_{\mathrm{P}}$ in equation (17). The third set of constraints in equation (17) are second-order cone constraints. In practice, the dual form of the above problem implemented as it is faster to solve. Figure 1 shows the deformation field of a point loaded clamped plate with $NE = 5000$. For the point loaded case, the dual objective function contains only one variable as opposed to $3NE = 15000$ in the primal problem, which is why the dual is more efficient to solve. The problem was set up in Matlab and solved using the commercial software package MOSEK [10], although several open source SOCP solvers are available and are also suitable.
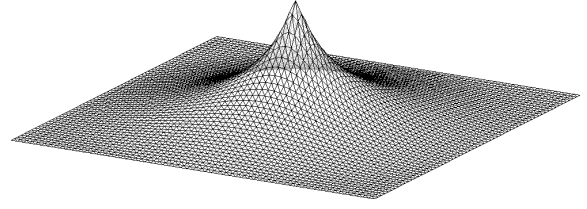

Fig. 1. Deformation field of point loaded sheet obtained by solving an upper bound plate problem using SOCP

B. Extension to shells

Unlike in plate theory, the finite elements that lie within a shell do not all share a common plane, but can instead be oriented arbitrarily in space with nodes at the global coordinates (X_i, Y_i, Z_i), for $i = 1, 2, 3$. The bending work for a particular element can be computed using the formulation in the previous section by defining velocities that operate within a local in-plane coordinate frame with respect to the element concerned. A transformation is then performed to align these velocities to the global reference frame. The coordinates in the local frame will be expressed by the lower case equivalents of the global system.

The membrane, or in-plane stretching, work component in a shell is now considered. Firstly, three further normalised stress resultants n_x, n_y and n_{xy} are introduced, which are defined as,

$$n_i = \frac{1}{N_o} \int_z \sigma_i dz, \quad i = x, y, xy, \tag{18}$$

where $N_o = \sigma_o h$ and σ_o is the material yield stress. The dissipation due to in-plane stretching is then given by

$$D_I = N_o \int_A n_x \dot{\epsilon}_x + n_y \dot{\epsilon}_y + n_{xy} \dot{\gamma}_{xy} \; dA, \tag{19}$$

where the strain rates are calculated from the in plane velocities u and v using the expressions,

$$\dot{\epsilon}_x = \frac{\partial u}{\partial x}, \quad \dot{\epsilon}_y = \frac{\partial v}{\partial y}, \quad \dot{\gamma}_{xy} = \frac{1}{2}\left(\frac{\partial u}{\partial y} + \frac{\partial v}{\partial x}\right). \tag{20}$$

A simple shell finite element is produced by superimposing a bending element, such as the BCIZ element, with a membrane element. Note that it has been assumed that the shell geometry can be suitably approximated by flat, rather than curved, triangular elements. In this case, the Allman element [11] is used to discretise the in-plane velocity fields and to compute membrane strains. As with the BCIZ element, this element has 9 degrees of freedom and three nodes, one at each vertex. The in-plane velocities u_i, v_i, and in-plane rotations $\theta_{z,i}$, are stored at each node $i = 1, 2, 3$. Within the local coordinate frame, the in-plane strains are related to these nodal velocities via a linear matrix relationship, so that for a node i of an element e within a finite element mesh,

$$\boldsymbol{\epsilon}_i^{(e)} = \mathbf{B}_{\mathrm{M},i}^{(e)}\mathbf{u}, \tag{21}$$

where $\boldsymbol{\epsilon}_i = [\dot{\epsilon}_{x,i} \ \dot{\epsilon}_{y,i} \ 2\dot{\tau}_{xy,i}]$, $\mathbf{B}_{\mathrm{M},i}^{(e)} \in \mathbb{R}^{3 \times NV}$ can be obtained from [11], and $\mathbf{u} \in \mathbb{R}^{NV}$ contains all of the in-plane variables for the element. Combining the plate and membrane components of strain [12],

$$\begin{bmatrix} \boldsymbol{\kappa}_i \\ \boldsymbol{\epsilon}_i \end{bmatrix} = \begin{bmatrix} \mathbf{B}_{\mathrm{P},i} & \mathbf{O} \\ \mathbf{O} & \mathbf{B}_{\mathrm{M},i} \end{bmatrix} \begin{bmatrix} \mathbf{w} \\ \mathbf{u} \end{bmatrix}, \qquad (22)$$

where the (e) superscripts have been ommitted for clarity. In order to relate the local variables $\mathbf{w}$ and $\mathbf{u}$ to a global coordinate frame, $\mathbf{W}$ and $\mathbf{U}$, a transformation matrix $\mathbf{T} = \mathbf{T}^{(e)}$ is computed for each element using the methodology outlined in [8]. Equation (22) can then be written as

$$\begin{bmatrix} \boldsymbol{\kappa}_i \\ \boldsymbol{\epsilon}_i \end{bmatrix} = \begin{bmatrix} \mathbf{B}_{\mathrm{P},i} & \mathbf{O} \\ \mathbf{O} & \mathbf{B}_{\mathrm{M},i} \end{bmatrix} \mathbf{T} \begin{bmatrix} \mathbf{W} \\ \mathbf{U} \end{bmatrix}. \qquad (23)$$

For the plate problem, the von Mises criterion was represented by the bending stress resultants only, but now the membrane components must also be incorporated. This can be done by using Ilyushin theory [13].

The Ilyushin criterion can be stated in terms of the quadratic stress intensities, Q_P, Q_M and Q_{MP},

$$Q_P = m_x^2 - m_x m_y + m_y^2 + 3m_{xy}^2, \qquad (24)$$
$$Q_M = n_x^2 - n_x n_y + n_y^2 + 3n_{xy}^2, \qquad (25)$$
$$Q_{MP} = n_x m_x - \frac{1}{2}(n_x m_y + n_y m_x) + n_y m_y + 3n_{xy} m_{xy}, \qquad (26)$$

or

$$Q_P = \mathbf{m}^T \mathbf{D} \mathbf{m}, \quad Q_M = \mathbf{n}^T \mathbf{D} \mathbf{n}, \quad Q_{MP} = \mathbf{n}^T \mathbf{D} \mathbf{m}, \qquad (27)$$

where,

$$\mathbf{m} = [m_x \ m_y \ m_{xy}]^T,$$
$$\mathbf{n} = [n_x \ n_y \ n_{xy}]^T,$$

and for the von Mises criterion,

$$\mathbf{D} = \begin{bmatrix} 1 & -\frac{1}{2} & 0 \\ -\frac{1}{2} & 1 & 0 \\ 0 & 0 & 3 \end{bmatrix} = \mathbf{R}^T \mathbf{R}. \qquad (28)$$

The Ilyushin criterion states that stress resultants must lie within the surface defined by the inequality [14]

$$Q_{MP}^2 \leq Q_P Q_M, \qquad (29)$$

which becomes an equality at yield, and is usually approximated by a linear equation that was also provided by Ilyushin,

$$Q_P + \frac{1}{\sqrt{3}}|Q_{MP}| + Q_M \leq 1. \qquad (30)$$

Equation (30) can be written in the form of two intersecting ellipsoids

$$\mathbf{s}^T \mathbf{Q}_1 \mathbf{s} \leq 1, \quad \mathbf{s}^T \mathbf{Q}_2 \mathbf{s} \leq 1, \qquad (31)$$

where $\mathbf{s} = [\mathbf{m}^T \mathbf{n}^T]^T$, $\mathbf{Q}_i$ is

$$\mathbf{Q}_i = \begin{bmatrix} \frac{\mathbf{D}}{M_0^2} & (-1)^{i-1}\frac{1}{2\sqrt{3}}\frac{\mathbf{D}}{M_0 N_0} \\ (-1)^{i-1}\frac{1}{2\sqrt{3}}\frac{\mathbf{D}}{M_0 N_0} & \frac{\mathbf{D}}{N_0^2} \end{bmatrix}, \qquad (32)$$

and $i = 1, 2$. From the principle of maximum plastic work,

$$\begin{aligned} d_I = \max_{\mathbf{s}} \ & \mathbf{s}^T \mathbf{\Phi}, \\ \text{s.t. } & \mathbf{s}^T \mathbf{Q}_1 \mathbf{s} \leq 1, \\ & \mathbf{s}^T \mathbf{Q}_2 \mathbf{s} \leq 1, \end{aligned} \qquad (33)$$

where $\mathbf{\Phi} = \begin{bmatrix} \boldsymbol{\kappa}^T & \boldsymbol{\epsilon}^T \end{bmatrix}^T$. The form of equation (33) is similar to the equivalent expression for the plate problem in equation (8), except there are two constraints representing the yield function rather than one. The problem cannot be treated analytically as in the plate problem, making the derivation of the SOCP more complicated. In order to simplify the above problem, a relaxation technique was applied to reduce the two constraints to a single constraint. This single constraint was chosen so that it optimally approximates the solution space given by the original two constraints. This was done by seeking an ellipsoid function of the form $\mathbf{s}^T \hat{\mathbf{Q}} \mathbf{s} \leq 1$ that best fits the intersection of the two ellipsoids in (31). The value of the approximation $\hat{\mathbf{Q}}$ was found by computing the ellipsoid of smallest volume that contains the intersection of the above constraints. Mathematically, if $\hat{e} = \{\mathbf{s}|\mathbf{s}^T \hat{\mathbf{Q}} \mathbf{s} \leq 1\}$, $e_i = \{\mathbf{s}|\mathbf{s}^T \mathbf{Q}_i \mathbf{s} \leq 1\}$ for $i = 1, 2$, then $\hat{e}$ is the smallest ellipsoid that it satisfies,

$$\hat{e} \supseteq \bigcap_{i=1}^{2} e_i. \qquad (34)$$

In this case, $\hat{e}$ is the so-called minimum outer ellipsoid. An alternative was also implemented, where $\hat{e}$ was approximated as the maximum inner ellipsoid, but this made little difference to the solution of the model and will not be discussed further. Both problems were cast as maximum determinant linear matrix inequality (LMI) optimisation problems using the procedure described by Boyd *et al* in [15], and solved for $\hat{\mathbf{Q}}$ using the semidefinite program solver, SeDuMi, details of which can be found in [16]. The resulting minimum outer ellipsoid is

$$\hat{\mathbf{Q}} = \mathbf{Q}_1 + \mathbf{Q}_2, \qquad (35)$$

which is closely related to approximations to the Ilyushin condition applied by other researchers, as discussed in [17]. The relaxed form of the principle of maximum plastic work is

$$\begin{aligned} d_I = \max_{\mathbf{s}} \ & \mathbf{s}^T \mathbf{\Phi}, \\ \text{s.t. } & \mathbf{s}^T \hat{\mathbf{Q}} \mathbf{s} \leq 1. \end{aligned} \qquad (36)$$

This can now be treated as before, and the internal dissipation can be cast as the integration over area of a norm by following the steps in equations (8) to (11). This can then be formulated as an SOCP problem after spatial discretisation.

The final optimisation problem is

$$D_I = \min \sum_i^{3NE} \frac{1}{3} z_i,$$

$$\text{s.t. } \boldsymbol{\eta} = \mathbf{PKTx},$$

$$\|\boldsymbol{\eta}_i\| \leq z_i, \quad i = 1, .., 3NE,$$

$$\mathbf{x}_{tool} \geq \text{Tool surface function},$$

$$\mathbf{x}_{boundary} = 0. \tag{37}$$

where $\boldsymbol{\eta}_i = [\eta_{1+6(i-1)}, \ldots, \eta_{6i}]$, $\mathbf{x} = [\mathbf{W}^T \ \mathbf{U}^T]^T$, $\mathbf{P}^T\mathbf{P} = \hat{\mathbf{Q}}$, and $\mathbf{K}$ is

$$\mathbf{K} = \begin{bmatrix} \Delta\mathbf{B}_{\mathbf{P},i}^{(e)} & \mathbf{O} \\ \mathbf{O} & \Delta\mathbf{B}_{\mathbf{M},i}^{(e)} \end{bmatrix} \mathbf{T}^{(e)}. \tag{38}$$

As with the plate problem, the edge boundary conditions can be implemented implicitly and as previously the tool constraints can be written as $\mathbf{Ex} \geq \mathbf{t}$. In practice, it is more efficient to solve the dual form of the problem.

Time integration is performed using a forward difference scheme to update the deformation field at each time step [4]. The time evolution of the model follows a sequential limit analysis [18] type scheme, which depends only on the change in position of the tool at each time step. An assumption about the contact conditions between the nodes of the finite element mesh and the tool is required for the $t+1$ time step. Specifically, it is assumed the nodes that coincide with the tool at time step t can only move vertically until time step $t+1$. This assumption is not strictly valid but is required to avoid the need for a time consuming iterative procedure to model the contact state between the tool and the sheet.

III. RESULTS

The model in this paper was verified against a part produced on the Cambridge AISF machine [19]. The test product, which is shown in fig. 2, was formed using 5251-H22 Aluminium alloy of 1mm thickness by the CNC tool-path displayed in fig. 3, reaching a maximum depth of 50mm and using a hemispherical tool with a radius of 10mm. The tool was tracked along at 10mm.s^{-1} over the 175mm×175mm sheet, which was clamped over a 140mm×140mm region. After the part was formed, 255 measurements were taken over the top surface of it using a coordinate measuring machine (CMM) and used for comparison against the model.

As with the plate problem, the model was solved using the SOCP software package MOSEK [10] for $NE = 5000$ on a standard desktop computer running MS Windows. The boundary conditions matched those above, and the solution was compared with the CMM measurements. These were superimposed over the model, and an interpolation field within each element was used to find the predicted deflection directly below, or above, each of the measured points. The results are shown in fig. 4, where the RMS vertical difference between measured and simulated data is 0.88mm, with a variance of 0.69mm^2 and maximum deflection of 3.17mm. The simulation took approximately 18 hours, with 60% of the time spent in the SOCP solver. The remaining period
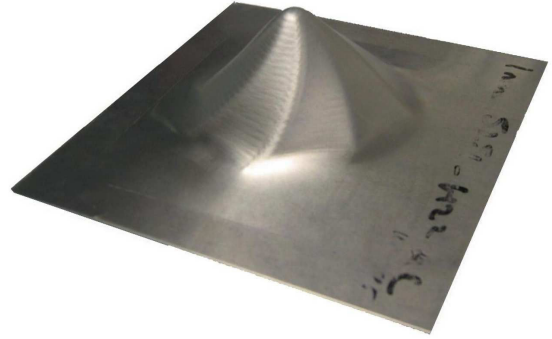

Fig. 2. Photograph of 5251-H22 Al alloy test product produced on the purpose built Cambridge AISF machine
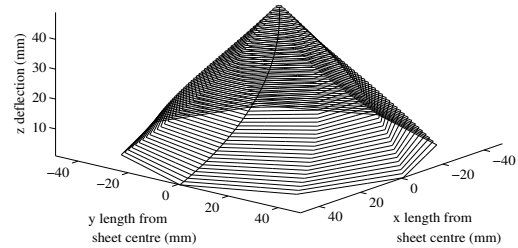

Fig. 3. The CNC tool path used to produce the product in fig. 2

was spent in matrix assembly and can be reduced by using a compiled script instead of Matlab. The lower limit on simulation time is 11 hours, the time spent in the solver.

This paper provides a first evaluation of the rigid plastic assumption for modelling ISF, and it uses recent SOCP methods when formulating the shell problem. Further work is required to observe the large reductions in computation time that have been obtained from applying the rigid plastic approximation to other processes [5]. It is not the intention of this paper to explore all these possibilities. However, one method, based on adaptive re-meshing, is displayed here, which reduced the solution time by 50% by halving NE to 2528, without affecting the predicted geometry. Specifically, a RMS vertical difference of 0.81mm was observed, with a variance of 0.65mm^2 and maximum deflection of 3.23mm when compared to the measured data. The idea was to use a coarse mesh that was refined within a region localised to the tool. As the tool moved, the refined region moved with it. Several remeshing algorithms were tried, of which the best was found to be based on a regular mesh with one degree of mesh refinement using the quadtree algorithm. The mesh generator used is implemented in the open source package, QMG [20]. The model used a base mesh that was generated over a 30×30 grid from which the localised region was refined to the equivalent of a 60×60 mesh, as displayed in
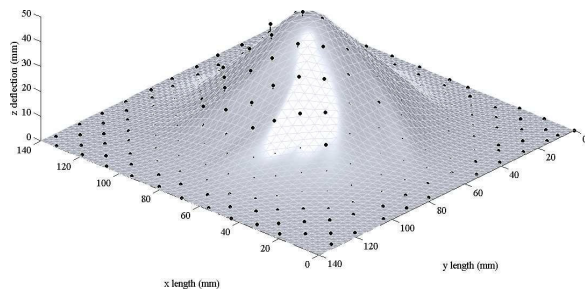
Fig. 4. Simulation of test product in fig. 2 produced by solving the rigid plastic shell problem using SOCP for a regular finite element mesh. The superimposed black dots are measured points from the real product.
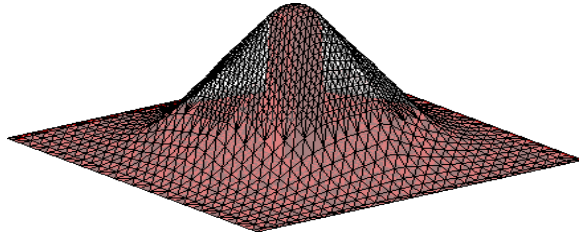

Fig. 5. Simulation of test product in fig. 2 produced by solving the rigid plastic shell problem using SOCP and mesh refinement around the tool. The tool is shown under the simulated sheet in its final position.

fig. 5.

IV. CONCLUSIONS AND FUTURE WORKS

A. Conclusions

This paper presents a model based on the rigid perfectly plastic assumption as a possible approximation in modelling incremental sheet forming (ISF). It is found to perform suitably in modelling product geometry when compared to a product formed on the Cambridge ISF machine. The paper firstly formulates the plate problem as a second-order cone program (SOCP). The model is then is extended by superposition of the plate problem with a membrane problem to simulate the plastic deformation of shells so that it can be used to model ISF. A relaxation of the linearised Ilyushin yield function is used to describe the yield surface in stress resultant space. This shell problem is also formulated as an SOCP. SOCP methods have recently gained interest as a possible technique for solving engineering problems, so this model is of a wider interest as a new example where SOCP has been applied to a modelling problem.

The simulation time is significantly shorter when compared to a full elastoplastic model, but it not short enough for real-time implementation. However, using a reasonably coarse mesh the model is currently suitable enough to run within an off-line tool path planning algorithm, which is in the form of a non-linear optimal control problem. The optimal control problem is currently being solved numerically using an outer optimisation algorithm that calls the model at each iteration step.

B. Future Works

The off-line optimal tool path will be tested on the ISF machine. Further model validation tests, including comparisons with commercial finite element software, are in progress and some modifications to improve the efficiency of the model are also being tested. Once computation times have been reduced to a satisfactory level, the off-line optimal control problem will be extended to a real-time model predictive control problem.

V. ACKNOWLEDGMENTS

REFERENCES

[1] J. Jeswiet, F. Micari, G. Hirt, A. Bramley, J. Duflou, and J. Allwood. Asymmetric single point incremental forming of sheet metal. *Annals of CIRP*, 54(2):623–650, 2005.

[2] J. M. Allwood, G. P. F. King, and J. Duflou. A structured search for applications of the incremental sheet-forming process by product segmentation. *Proc. Inst. of Mech. Eng. Part B: J. Engineering Manufacture*, 219:239–244, 2005.

[3] A. Raithatha, K. Jackson, S. Duncan, and J. Allwood. New method for modeling plastic deformation in incremental sheet forming. *Proc. IEEE CCA*, 2006.

[4] A. Raithatha, S. Duncan, K. Jackson, and Julian Allwood. Second order cone programming in modeling incremental deformation. *Proc. 26th American Control Conf.*, 2007.

[5] M. J. Sharan. Comparison of elastic-plastic and rigid-plastic implicit FEM simulations in sheet forming applications. *Journal of Materials Processing Technology*, 27:279–300, 1991.

[6] E. Christiansen. Limit analysis for plastic plates. *Siam. J. Math. Anal.*, 11:514–522, 1980.

[7] K. D. Anderson, E. Christiansen, and M. Overton. Computing limit loads by minimising the sum of norms. *SIAM J. Sci. Comput.*, 19:3, 1998.

[8] O. C. Zienkiewicz and R. L. Taylor. *The Finite Element Method for Solid and Structural Mechanics, 5th edition.* Butterworth-Heinemann, 2000.

[9] C. A. Felippa. Web-posted lectures on advanced finite element methods, at http://caswww.colorado.edu/courses.d/afem.d/home.html.

[10] MOSEKApS. *The MOSEK optimization toolbox for MATLAB version 3.2 (Revision 8). User's guide and reference manual.* MOSEK ApS. Denmark., 2002.

[11] D. J. Allman. A compatible triangular element including vertex rotations for plane elasticity analysis. *Computers and Structures*, 19:1–8, 1984.

[12] R. D Cook, D. S. Malkus, M. E. Plesha, and R. J. Witt. *Concepts and applications of Finite Element Analysis, 4th edition.* John Wiley & Sons, 2002.

[13] A. A. Ilyushin. Plasticité. *(in French) Editions Eyrolles, Paris*, 1956.

[14] C. J. Burgoyne and M. G. Brennan. Exact Ilyushin yield surface. *Int. J. Solids and Structures*, 30:1113–1131, 1993.

[15] S. Boyd, L. El Ghaoui, E. Feron, and V. Balakrishnan. *Linear Matrix Inequalities in System and Control Theory.* SIAM, 1994.

[16] H. D. Mittelmann. An independent benchmarking of SDP & SOCP solvers. *Math. Prog.*, 95:407–430, 2003.

[17] Q. Zeng, A. Combescure, and F. Arnaudeau. An efficient plasticity algorithm for shell elements application to metal forming simulation. *Computers and Stuctures*, 79:1525–1540, 2001.

[18] Wei H. Yang. Large deformation of structures by squential limit analysis. *Int. J. Solids Structures*, 30(7):1001–1013, 1993.

[19] J. M. Allwood, N. E. Houghton, and K. P. Jackson. The design of an incremental sheet forming machine. *SheMet '05*, 2005.

[20] Mitchell and S. Vavasis. Quality mesh generation in higher dimensions. *SIAM J. Comput.*, 29:1334–1370, 2000.